Cucurbit[8]uril templated supramolecular ring structure formation and protein assembly modulation

Please check the document version of this publication:

• A submitted manuscript is the version of the article upon submission and before peer-review. There can be important differences between the submitted version and the official published version of record. People interested in the research are advised to contact the author for the final version of the publication, or visit the DOI to the publisher's website.
• The final author version and the galley proof are versions of the publication after peer review.
• The final published version features the final layout of the paper including the volume, issue and page numbers.

[Link to publication](#)

Cucurbit[8]uril templated supramolecular ring structure formation and protein assembly modulation†

Mellany Ramaekers,‡[ab] Sjors P. W. Wijnands,‡[ab] Joost L. J. van Dongen,[ac] Luc Brunsveld[ab] and Patricia Y. W. Dankers*[ab]

The interplay of Phe-Gly-Gly (FGG)-tagged proteins and bivalent FGG-tagged penta(ethylene glycol) as guest molecules with cucurbit[8]uril (Q8) hosts is studied to modulate the supramolecular assembly process. Ring structure formation of the bivalent guest molecule with Q8 leads to enhanced binding properties and efficient inhibition of protein assemblies.

Supramolecular systems are regularly used regarding their reversibility, dynamic interactions with biomolecules and easy modification *via* non-covalent synthesis.[1] Directional non-covalent interactions such as hydrogen bonding and host–guest interactions have the advantage of specificity and tunability.[2] This is reflected in recent research on the co-assembly of peptides and organic compounds yielding new interesting properties.[3] Host–guest assemblies based on cyclodextrin and cucurbit[*n*]uril have been shown to form stable complexes with varying degrees of selectivity and reversibility.[4] Cucurbit[8]uril (Q8) is a donut shaped host, which can bind two guests in its cavity.[5] Using bivalent guests this Q8 binding can lead to supramolecular polymerization. Ring–chain equilibrium effects depend on the system properties and are an important factor to take into account in this matter.[6] Urbach *et al.* revealed the Q8 recognition of tripeptide guests like Phe-Gly-Gly (FGG) and Trp-Gly-Gly (WGG).[7] The ability of Q8 to selectively dimerize FGG and WGG motifs was subsequently used for the reversible dimerization of proteins.[8] Using the short FGG-tag, a recent study showed the dimerization and activation of two caspase proteins by Q8 and the

inhibition of this active casp-9 dimer by FGG peptides as competitor molecules.[9] Here, we report on a well-defined bifunctional penta(ethylene glycol) modified with two FGGG-motifs that efficiently forms a stable ring-structure with Q8 and effectively modulates protein assembly (Fig. 1). We have chosen the combination of a penta(ethylene glycol) linker with two times three glycines because reconstruction (using Pymol) indicated minimal physical hindrance of this linker on the formation of ring structures. A variety of experimental techniques reveals the enhanced complexation behavior and underlying thermodynamic parameters, and the interplay of interactions of FGG-tagged proteins and the bivalent inhibitor with Q8.

For the construction of the (FGGG)$_2$–penta(ethylene glycol) molecule (compound **1**, Fig. 1a), solid phase peptide synthesis on Wang resin was applied yielding Fmoc-protected FGGG (0.7 g, 75%, ESI,† Scheme S1). In a next step, the Fmoc-protected FGGG was activated with 0.95 eq. HBTU in solution and 0.25 eq.
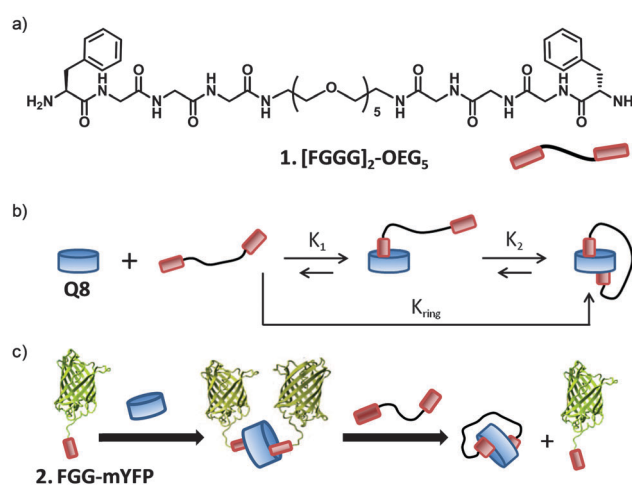
^{a} Institute for Complex Molecular Systems, Eindhoven University of Technology,
P.O. Box 513, 5600 MB Eindhoven, The Netherlands.
E-mail: p.y.w.dankers@tue.nl

^{b} Laboratory of Chemical Biology, Department of Biomedical Engineering,
Eindhoven University of Technology, P.O. Box 513, 5600 MB Eindhoven,
The Netherlands

^{c} Laboratory of Macromolecular and Organic Chemistry,
Department of Chemical Engineering, Eindhoven University of Technology,
P.O. Box 513, 5600 MB Eindhoven, The Netherlands

† Electronic supplementary information (ESI) available: Experimental section, ^{1}H-NMR, ITC, reaction equilibria, DOSY-NMR, SEC, QTOF-MS, MALDI-TOF MS, FGG-mYFP sequence, fluorescence anisotropy. See DOI: 10.1039/c4cc08917k

‡ Joint first authors.

Fig. 1 (a) Chemical structure of the bivalent penta(ethylene glycol) peptide (compound **1**). (b) The formation of a 1:1 ring structure of Q8 and **1** described by the overall binding constant K_{ring} and the inter- and intramolecular binding constants K_1 and K_2. (c) Protein dimerization *via* Q8 complexation and protein disassembly *via* ring formation of **1** and Q8.

OEG$_5$–diamine was added to yield Fmoc-protected compound **1** (ESI,† Scheme S2). Fmoc deprotection, with 0.7 eq. DBU and a 10-fold excess of 1-octanethiol, followed by purification using preparative LCMS yielded pure compound **1**.

To investigate complex formation between bivalent compound **1** and Q8, ^{1}H-NMR experiments were performed (Fig. 2a). The up-field shift of the aromatic protons of the phenylalanines was clearly visible when Q8 was added in a 1:1 ratio to **1** in D$_2$O. The absence of the aromatic peak signals in the range of 7.44 to 7.30 ppm furthermore indicates that all FGGG-motifs are bound in the cavity of Q8. Furthermore, either heating of the 1:Q8 complex from 10 to 70 °C, or addition of base or acid did not show a change in complexation (i.e. no down-field shift of the aromatic protons of Phe was observed), indicating no responsive to temperature and pH (ESI,† Fig. S3 and S4).

With DOSY-NMR, the complexation of Q8 with compound **1** was studied. The diffusion coefficient of the 1·Q8 complex reveals the formation of rings or chains. The diffusion coefficient of the complexes was determined at differing 1:Q8 ratios, varying from 0.5:1 to 3:1 (ESI,† Fig. S7). Next to this, the diffusion coefficient was determined for pure Q8 and over a range of concentrations of a 1:1 Q8:1 mixture from 10 μM to 1 mM (Fig. 2b). Addition of compound **1** to Q8 results in a 1.7 times smaller diffusion coefficient due to

Fig. 2 (a) ^{1}H-NMR spectra of **1** at 100 μM in D$_2$O (red) and a 1:1 mixture of Q8 and compound **1** at 100 μM in D$_2$O (blue). An up-field shift is visible after complexation of the phenyl-groups in Q8, showing that compound **1** is bound. (b) Average diffusion coefficient of Q8 at different concentrations in 1:1 mixtures with **1** (except for the measurement at 0 μM **1**, which denotes pure Q8 at 100 μM), determined by DOSY-NMR.

complex formation. Using the Stokes–Einstein equation[10] and the determined diffusion coefficients, an estimate of the hydrodynamic radius (R_H) for a spherical particle can be made. The diffusion coefficient of Q8 is 3.35×10^{-10} m^2 s^{-1} and the R_H is 5.94 Å, which is in the same range of the known dimensions of Q8; 9.1 Å in height and 17.5 Å in width.[11] The 1·Q8 complex has an average diffusion coefficient of 2.03×10^{-10} m^2 s^{-1} and the R_H is 9.81 Å, thus an increase in size is observed for complex formation. The absence of a significant change in diffusion coefficient between different concentrations of the supramolecular complex indicates that one single species, a ring structure, is formed and that there is no formation of larger complexes over this concentration range. Even at a concentration of 1 mM of both compounds no changes in the diffusion coefficient are observed indicative of chain-like supramolecular assemblies. This shows that the ring–chain equilibrium is fully directed to ring formation for this molecular system.

Based on previous research by Urbach et al.,[7a] the binding stoichiometry of the bivalent **1** to Q8 can be hypothesized to be one. The formation of this complex can be described by the overall binding constant $K_{ring} = ([Q8·1_2])/([Q8]·[1])$ (eqn (S1), ESI†). In a ring–chain equilibrium the formation of ring structures is dependent on the effective concentration (C_{eff}) and the total concentration of the system.[12] The binding process for ring formation can be described by a two-step process with binding constant K_1 representing the intermolecular binding of the first FGGG-motif of **1** in the cavity of Q8 and K_2 the intramolecular binding of the second FGGG of **1** (Fig. 1b). K_2 is dependent on the C_{eff} as described in $K_2 = K_1·C_{eff}$ (eqn (S2), ESI†).[6a,12] Integrating eqn (S1) into eqn (S2) (ESI†) provides $K_{ring} = K_{ter}·C_{eff}$ (eqn (S3), ESI†), with K_{ter} being the binding constant of two FGGG peptides complexed in Q8 (ESI,† Fig. S5 and Table S1).§

ITC experiments with Q8 and **1** were performed and the resulting data were fitted with a one set of sites binding model,[13] since the second binding involved is presumed to be an intramolecular binding (Fig. 3a, ESI,† Table S1). With this model, the binding stoichiometry was determined to be one, as expected. This is in agreement with the NMR data showing a binding ratio of compound **1** to Q8 of 1:1. K_{ring} was determined to be 9.0×10^6 M^{-1}. This affinity is a significant improvement in comparison to the two-fold binding of two separate FGG motifs, showing the effectiveness of the linker in enhancing the affinity for Q8. Using eqn (S3) (ESI†), the effective concentration was calculated to be 750 μM. The enthalpy values for the binding of monovalent FGGG **3** and **1** are comparable, which indicates that there is little to no steric effect of the OEG$_5$ linker on the binding of the FGGG-motifs in Q8.

QTOF-MS was used to further determine the molecular characteristics of the formed ring complexes. A solution of either **1** or a 1:1 mixture of Q8 and **1** were measured (ESI,† Fig. S9 and Fig. 3b). The deconvoluted spectrum of the 50 μM 1:1 mixture of Q8 and **1** clearly demonstrates that the Q8·**1** 1:1 complex is predominantly formed, with a calculated [M + H]$^+$ of 2246.5 g mol^{-1} (ESI,† Fig. S9b). Apart from this complex, in minor quantities also Q8$_2$·**1** was detected, with a calculated [M + Na]$^+$ of 3597.6 g mol^{-1}, as well as free **1**, with a [M + Na]$^+$ of 939.4 g mol^{-1}. No supramolecular polymer chains or ring structures containing multiple units were detected at this concentration. To confirm the findings of the
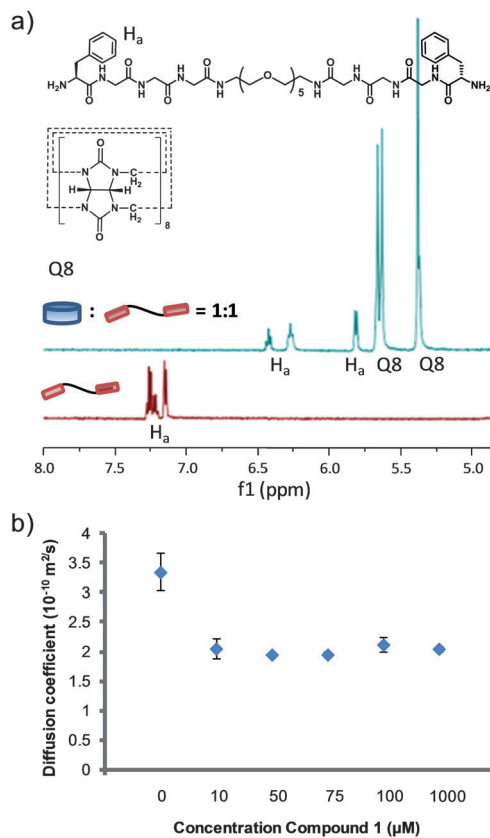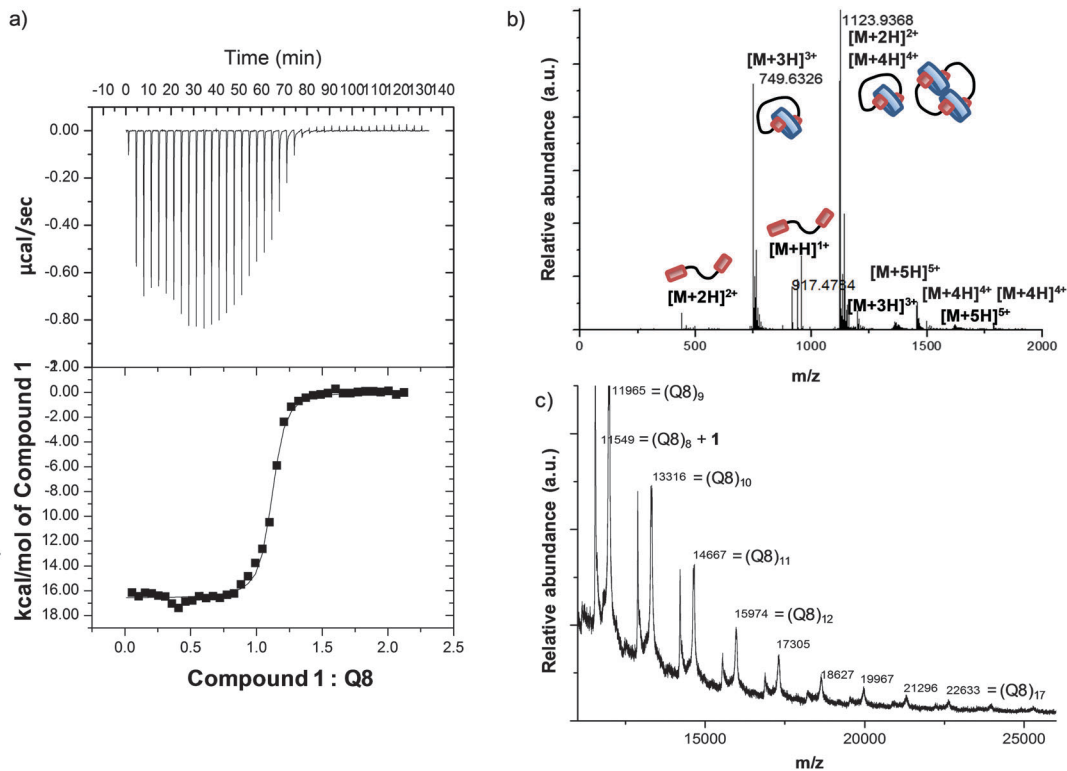
Fig. 3 (a) ITC titration of **1** at 500 μM to Q8 at 50 μM in 10 mM pH 7 sodium phosphate buffer at 27 °C. Top: raw data of power *versus* time. Bottom: integrated enthalpy *versus* the molar ratio. The fitted data provide a stoichiometry of 1.09, an association constant of 9.0×10^6 M^{-1} and a change in enthalpy of −69.5 kJ mol^{-1} (−16.6 kcal mol^{-1}), further thermodynamic parameters can be found in ESI,† Table S1. (b) QTOF-MS spectrum of a 1 mM 1:1 mixture of **1** and Q8, the predominantly present complexes are the Q8·**1** complex with a calculated $[M + 3H]^{3+}$ of 749.5 g mol^{-1}, and $[M + 2H]^{2+}$ of 1123.8 g mol^{-1}. (c) MALDI-TOF MS spectrum of a 1:1 Q8:**1** at 2 mM (filtered) solution in water. Detected masses are equal to Q8 aggregated species (broad peaks) and Q8 aggregated species with one compound **1** (sharp peaks).

DOSY-NMR experiments at higher concentrations, a 1 mM solution of Q8 and **1** was analyzed by QTOF-MS as well. As seen in the mass spectrum in Fig. 3c the predominant complex present is again the 1:1 complex of Q8 and **1** (calculated $[M + 3H]^{3+}$ = 749.5 g mol^{-1} and $[M + 2H]^{2+}$=1123.8 g mol^{-1}). Next to this at minor amounts, free **1**, and some additional larger species were detected which could be assigned to the 2:2, 2:1, 3:2, 3:3 and 4:3 (Q8:**1**) complexes. The results show that 1:1 rings are predominantly formed and only at the very high mM concentrations, also some other higher order species occur.

MALDI-TOF-MS out of a solid matrix revealed masses up to 25 000 g mol^{-1} (Fig. 3c). However, the observed mass pattern exactly correlates with Q8 aggregates for the broad signal, and Q8 aggregates with only one compound **1** bound for the sharper signals. For example, the mass of 22 633 g mol^{-1} equals exactly 17 Q8 molecules. Also at a dilute concentration, the same pattern of Q8 aggregation is observed. Confirming DOSY-NMR results, it can be concluded that no supramolecular polymers are formed between Q8 and **1**. Next to that, the aggregation observed is an artifact of MALDI-TOF MS, an event known to occur with specific ionization conditions. Recent published data by Zhang *et al.* on a bifunctional FGG peptide with an octa(ethylene glycol) spacer, (FGG)$_2$–OEG$_8$[14] use MALDI-TOF to conclude that supramolecular polymers with a high polymerization degree are formed. MALDI-TOF MS measurement of **1** and Q8 showed a similar pattern as published for (FGG)$_2$–OEG$_8$, indicating that the published data likely result from the artifact Q8 oligomers as well.

Finally, we evaluated the inhibiting properties of the newly developed bivalent guest **1** on protein assembly. Fluorescence anisotropy studies were performed to study the host–guest behavior and complexation of Q8 complexes with FGG-tagged monomeric yellow fluorescent protein (**2**) in response to **1**. YFP proteins dimerized *via* Q8 show efficient homo-FRET.[15] Based on the ITC data, we hypothesized that the binding of **1** to Q8 is more favorable than the formation of a ternary complex of Q8 with FGG-mYFP. Titration of **1** to the Q8:**2** complex indeed resulted in the return of the anisotropy value to that corresponding to free FGG-mYFP. Only one equivalent of **1** sufficed to fully block the protein assembly, which confirms that binding of Q8 to **1** is energetically more favorable than twofold binding of FGG-mYFP in Q8. In contrast to **1**, monofunctional FGGG **3** required a large excess to inhibit the protein assembly (Fig. 4b).

The competition between a premade Q8·**1** ring and **2** was studied and further corroborated that the binding of the ring complex of **1** and Q8 is stronger than the binding of the dimerized proteins (Fig. 4c).

Titration of Q8, to a 2:1 mixture of FGG-mYFP and **1**, shows that only upon depletion of **1**, Q8 binds to the protein to form the protein complex with corresponding homo-FRET (Fig. 4d). The results highlight the preference for the binding of compound **1** in Q8 over
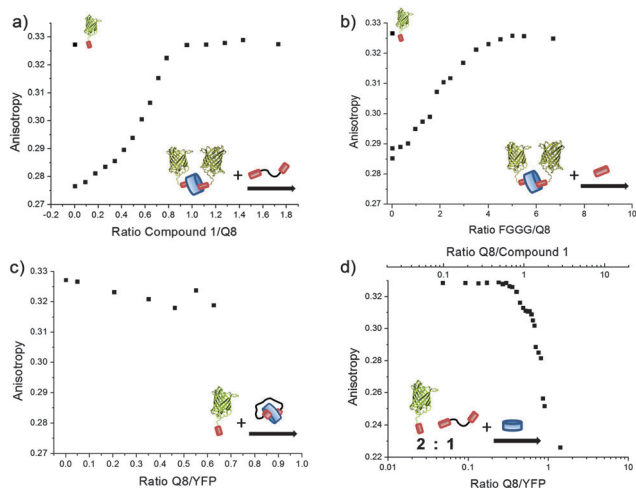
Fig. 4 Fluorescence anisotropy measurements of (a) a 2 μM FGG-mYFP solution, adding 4.5 μM Q8 solution in a second step followed by a titration of **1**, (b) a 2 μM FGG-mYFP solution, adding 4.5 μM Q8 solution in a second step followed by a titration of FGGG peptide, (c) a 2 μM FGG-mYFP solution and a titration of complexed Q8 with **1** in a 1 : 1 ratio, (d) a solution of 2 μM FGG-YFP and 1 μM **1** and a titration of Q8.

the protein and clearly show that in the ring regime, compound **1** acts as a very efficient protein assembly inhibitor.

The defined ring structure of (FGGG)$_2$–OEG$_5$ and Q8, with the high K_{ring} thus provides a more efficient inhibition of the protein assembly compared to simple FGGG peptides. The effective concentration of the peptides in the bivalent guest determines the position of the ring–chain equilibrium. By increasing the valency of the guest molecule, the increase of identical nearby guests adds a statistical term to the equation which is likely to result in an even bigger preference for the formation of ring structures and hence, an even stronger inhibitor.[16] The results shown open up the possibility for controlled release or switching of protein assemblies within supramolecular systems.

Notes and references

§ The complete derivation of the shown equations and the used reaction equilibria can be found in the supporting info Section 4.

1 (a) G. A. Silva, C. Czeisler, K. L. Niece, E. Beniash, D. A. Harrington, J. A. Kessler and S. I. Stupp, *Science*, 2004, **303**, 1352–1355; (b) L. W. Chow, R. Bitton, M. J. Webber, D. Carvajal, K. R. Shull, A. K. Sharma and S. I. Stupp, *Biomaterials*, 2011, **32**, 1574–1582; (c) J. Li and X. J. Loh, *Adv. Drug Delivery Rev.*, 2008, **60**, 1000–1017; (d) K. H. Smith, E. Tejeda-Montes, M. Poch and A. Mata, *Chem. Soc. Rev.*, 2011, **40**, 4563–4577; (e) A. González-Campo, B. Eker, H. J. G. E. Gardeniers, J. Huskens and P. Jonkheijm, *Small*, 2012, **22**, 3531–3537.

2 J. Cabanas-Danés, J. Huskens and P. Jonkheijm, *J. Mater. Chem. B*, 2014, **2**, 2381–2394.

3 (a) X. Huang, M. Li, D. C. Green, D. S. Williams, A. J. Patil and S. Mann, *Nat. Commun.*, 2013, **4**, 2239; (b) Q. Zou, L. Zhang, X. Yan, A. Wang, G. Ma, J. Li, H. Möhwald and S. Mann, *Angew. Chem., Int. Ed.*, 2014, **53**, 2366–2370.

4 (a) J.-H. Seo, S. Kakinoki, Y. Inoue, T. Yamaoka, K. Ishihara and N. Yui, *J. Am. Chem. Soc.*, 2013, **135**, 5513–5516; (b) A. E. Kaifer, *Acc. Chem. Res.*, 2014, **47**, 2160–2167; (c) W. S. Jeon, K. Moon, S. H. Park, H. Chun, Y. H. Ko, J. Y. Lee, E. S. Lee, S. Samal, N. Selvapalam, M. V. Rekharsky, V. Sindelar, D. Sobransingh, Y. Inoue, A. E. Kaifer and K. Kim, *J. Am. Chem. Soc.*, 2005, **127**, 12984–12989.

5 (a) H.-J. Kim, J. Heo, W. S. Jeon, E. Lee, J. Kim, S. Sakamoto, K. Yamaguchi and K. Kim, *Angew. Chem., Int. Ed.*, 2001, **40**, 1526–1529; (b) W. S. Jeon, H.-J. Kim, C. Lee and K. Kim, *Chem. Commun.*, 2002, 1828–1829; (c) V. Sindelar, M. A. Cejas, F. M. Raymo, W. Chen, S. E. Parker and A. E. Kaifer, *Chem. – Eur. J.*, 2005, **11**, 7054–7059.

6 (a) G. Ercolani, *J. Am. Chem. Soc.*, 2003, **125**, 16097–16103; (b) H. W. Gibson, N. Yamaguchi and J. W. Jones, *J. Am. Chem. Soc.*, 2003, **125**, 3522–3533; (c) M. M. C. Bastings, T. F. A. de Greef, J. L. J. van Dongen, M. Merkx and E. W. Meijer, *Chem. Sci.*, 2010, **1**, 79–88.

7 (a) L. M. Heitmann, A. B. Taylor, P. J. Hart and A. R. Urbach, *J. Am. Chem. Soc.*, 2006, **128**, 12574–12581; (b) P. Rajgariah and A. R. Urbach, *J. Inclusion Phenom. Macrocyclic Chem.*, 2009, **62**, 251–254; (c) J. J. Reczek, A. A. Kennedy, B. T. Halbert and A. R. Urbach, *J. Am. Chem. Soc.*, 2009, **131**, 2408–2415.

8 H. D. Nguyen, D. T. Dang, J. L. J. van Dongen and L. Brunsveld, *Angew. Chem., Int. Ed.*, 2010, **49**, 895–898.

9 D. T. Dang, H. D. Nguyen, M. Merkx and L. Brunsveld, *Angew. Chem., Int. Ed.*, 2013, **52**, 1–6.

10 (a) A. Einstein, R. Furth and A. D. Cowper, *Investigations on the Theory of the Brownian Movement*, Courier Dover Publications, Mineola, NY, 1956; (b) S. Floquet, S. Brun, J.-F. Lemonnier, M. Henry, M.-A. Delsuc, Y. Prigent, E. Cadot and F. Taulelle, *J. Am. Chem. Soc.*, 2009, **131**, 17254–17259.

11 J. Kim, I.-S. Jung, S.-Y. Kim, E. Lee, J.-K. Kang, S. Sakamoto, K. Yamaguchi and K. Kim, *J. Am. Chem. Soc.*, 2000, **122**, 540–541.

12 V. M. Krishnamurthy, V. Semetey, P. J. Bracher, N. Shen and G. M. Whitesides, *J. Am. Chem. Soc.*, 2007, **129**, 1312–1320.

13 *ITC Data Analysis in Origin Tutorial Guide Version 7.0*, MicroCal, LLC, 2004.

14 X. Tan, L. Yang, Y. Liu, Z. Huang, H. Yang, Z. Wang and X. Zhang, *Polym. Chem.*, 2013, **4**, 5378–5381.

15 D. W. Piston and G.-J. Kremers, *Trends Biochem. Sci.*, 2007, **32**, 407–414.

16 G. Ercolani and L. Schiaffino, *Angew. Chem., Int. Ed.*, 2011, **50**, 1762–1768.